Hybrid nanocomposites of a fluorescent block copolymer and quantum dots: An efficient way for energy transfer

I. Moura*, A. de Sá**, Ana S. Abreu, M. Oliveira, A.V. Machado

Institute of Polymers and Composites (IPC) and Institute of Nanostructures, Nanomodelling and Nanofabrication (i3N), University of Minho, Campus de Azurém, 4800-058, Guimarães, Portugal

Keywords:

Polymer synthesis
Fluorescent block copolymer
Quantum dots
Hybrid nanocomposites
FRET

Abstract

Förster resonance energy transfer (FRET) phenomenon has great potential in several applications, whose efficiency is dependent on the energy transfer between a suitable pair of fluorophores. In this work, a new block copolymer, PS-b-PS(co-pyren-1-yl), with fluorescent properties, was synthetized and used as donor component in the fluorophores pair copolymer/cadmium telluride quantum dots (CdTe QDs). Thus, water-soluble CdTe QDs, previously transferred into organic phase, by replacing the stabilizer ligands, thioglycolic acid by 1-dodecanethiol (1-DDT), were used to prepare a new hybrid nanocomposite. FRET studies between the fluorescent copolymer and CdTe-DDT QDs revealed that this fluorophores pair can experience FRET with an efficiency of 48%, being an efficient antenna system for light harvesting applications.

Introduction

Quantum dots (QDs) have attracted high research attention due to their importance in different research fields, including imaging, manufacture of chemical sensors, optical switches, biomedical fluorescent probes and light harvesting [1,2]. QDs should have good

chemical stability, in order to preserve their initial fluorescence efficiency. Therefore, it is of high concern to prevent nanoparticles (NPs) aggregation and agglomeration, which can be achieved with a suitable organic ligand as surface capping [3-5]. The synthesis of QDs in aqueous medium is a simple, less toxic and a more reproducible approach, allowing their scale-up production [6].

Cadmium telluride (CdTe) QDs have attracted great interest due to their high Φ_F and size-dependent emission in the visible range of the electromagnetic spectrum [7]. The conjugation of excellent optical and physicochemical properties of polymers with fluorescent QDs allows to develop new nanocomposite materials with improved processability, along with enhanced colloidal and thermal stability of the NPs derived from the interaction with the

polymers [8,9]. Nevertheless, in order to disperse the hydrophilic CdTe QDs in a common polymer matrix, chemical compatibility is required. It is, thus, essential to modify their hydrophilic surface [10], preserving or enhancing their Φ_F and chemical stability.

When conjugated with a suitable fluorophore [11], QDs can be useful for applications in which energy transfer is essential, for instance via Förster resonance energy transfer (FRET) [10,12,13]. FRET is as a non-radiative energy transfer pathway, from an excited donor to a ground-state acceptor, through dipole-dipole interactions, that requires spectral overlap and close proximity between a donor and an acceptor [14]. A distance among the fluorophores pairs, between 2 and 10 nm , is crucial for the FRET efficiency [15]. Thus, a spatial requirement could be employed for judging the respective distance between both [16]. Furthermore, according to Förster theory, the rate of energy transfer is also dependent on Φ_F of the donor [17]. Fluorophores pairs based on QD-QD, organic dye-organic dye and QD-organic dye are found in literature as FRET systems [18], with higher incidence on those based on organic dies [19].

FRET studies involving CdTe QDs are reported in the literature. Higgins et al. [20] demonstrated that CdTe QDs with oppositely charged ligands formed nanoclusters, where the smaller QDs act as donors and the larger as acceptors within the clusters, having a FRET efficiency of 45%. Lin et al. [21] showed that FRET in a mixedsize CdTe QDs films is quite dependent on donor and acceptor (D/A) concentration ratios. Other studies reporting FRET efficiency between CdTe QDs, with different sizes, and Rhodamine B (RhB), an organic dye, were carried out [22]. Herein, it was also shown that D/ A ratio and FRET efficiency are closely linked. Even though several studies have shown that CdTe QDs act effectively as donors in FRETbased systems, other organic/inorganic fluorophores could also be promising [23]. According to Förster theory, they are able to transfer energy to QD acceptors and therefore, achieve suitable FRET efficiency.

FRET has been applied in photoconversion devices, as a conceivable energy transfer mechanism in light harvesting assemblies [24]. Besides the electronic energy transfer capacity, an antenna systems should also be able to absorb light with high efficiency [25]. Polymers or block copolymers based on monomers with fluorescent properties, have appropriate photo and thermostability and can be used as colored polymers resistant to solvents and migration [26,27].

Despite of many types of fluorescent materials have been combined with CdTe QDs to produce FRET-capable systems, there are few publications regarding the energy transfer between a fluorescent polymer and semiconductor CdTe QDs.

Rogach [28], reported a photophysical study of a hybrid watersoluble composite of a conducting copolymer, poly [9,9-bis ($3' - ((N,N$-dimethyl)- N-ethylammonium)-propyl)-2,7-fluorene-alt-1,4phenylene] dibromide - PDFD, and CdTe QDs capped with 2-sulfanylacetic acid (SAA), that showed efficient energy transfer from PDFD to the NPs. More recently, Huang et al. [10] reported the synthesis of a high fluorescent polymer composites based on the chemical bonding of CdTe QDs (CdTe-CPA) and a 1,8-naphthalimide derivative (N-CPA) to polyacrylate (CPA). The authors successfully observed resonance energy transfer from the donor (N-CPA), to the acceptor (CdTe-CPA).

This work aims to develop a new fluorescent copolymer, PS-b-PS(co-pyren-1-yl), suitable for a proper dispersion of hydrophobic QDs and, at the same time, produce an efficient fluorophores pair for energy transfer through FRET. Pyrene is a well-known fluorophore with wide application in the electronics filed [29]. Since its emission is centered below 500 nm [30], it is foreseen a fluorophore pair in which the polymer acts as the energy donor, overlapping the absorption spectrum of hydrophobic QDs that act as the acceptor.

The block copolymer was synthesized by a strategy combining reversible addition-fragmentation transfer (RAFT) and palladiumcatalyzed Suzuki cross coupling. Water soluble CdTe-SAA QDs were chemically modified to CdTe capped with 1-dodecanethiol (1DDT), using a ligand exchange methodology [31], to obtain organic soluble NPs. Then, by dispersing CdTe-DDT QDs, with a maximum emission wavelength of 543 nm , within a solution of PS-b-PS(co-pyren-1-yl) ($\lambda_{em} = 425$ nm), we prepared a suitable QD-dye fluorophores pair that can experience FRET. The Φ_F for the individual components was determined and FRET was investigated for the resulting hybrid nanocomposite, as well as its morphology and thermal stability. Our results suggest that this hybrid material might be a suitable antenna for light harvesting applications.

Experimental

Materials

Benzyl benzodithioate (BDTB, 96%), 2,2'-azobis(2methylpropionitrile) (AIBN, 98%), pyrene 1 -boronic acid ($\geq$ 95%), 1-dodecanethiol (1-DDT, $\geq$ 98%), and CdTe-SAA ($\lambda_{em} =$ 520 nm) were acquired to Sigma-Aldrich. Styrene (99.5%), 4-bromostyrene (4BrS, 96%), and bis(triphenylphosphine) palladium(II) chloride [$PdCl_2(PPh_3)_2$, 98%], were purchased to Acros Organics. Potassium carbonate anhydrous (K_2CO_3, 99.7%), N,N-dimethylformamide
(DMF, 99.9%), tetrahydrofuran (THF, 99.9%), petroleum ether $40 - 60\ ^\circ C$, chloroform ($CHCl_3$, $\geq$ 99.9%), ethyl acetate (99.99%), acetone (99.98%), and diethyl ether (99.99%) were obtained from Fisher Chemical. Methanol (MeOH, 99.9%) and magnesium sulphate anhydrous ($MgSO_4$) were purchased to Panreac. All chemicals were used as received.

Synthesis of PS-b-P4BrS

Typically, into a 25 mL Schlenk tube, PS macroRAFT (0.996 g , 0.222 mmol), prepared accordingly to the procedure described by Abreu et al. [32], 4BrS (1.0 mL, 7.65mmol) and AIBN (0.009 g , 0.055 mmol) were dissolved in DMF (10 mL), in the ratio PS macroRAFT: AIBN: 4BrS = 1: 0.25 : 34 . The mixture was degassed and placed under nitrogen atmosphere. After 42 h of reaction at $110^\circ C$, the tube was cooled to room

temperature immediately. The reaction mixture was evaporated under reduced pressure and the crude obtained redissolved in a small amount of THF. The block copolymer (PS-***b*** **– P4BrS**) was obtained by precipitation in MeOH as a light pink solid (1.467 g). ^{1}H NMR (400MHz, $CDCl_3$): 1.20-1.75 (broad m, aliphatic protons), 1.78-2.15(broad m, aliphatic protons), 6.10-6.75 (broad m, ArH), 6.90-7.35 (broad m, ArH) ppm. Mn (GPC) 8410 g^{-1}, Mw (GPC) 9589 g^{-1} with a polydispersity index (PDI) of 1.14 .

Synthesis of PS-b-PS(co-pyren-1-yl)

Pyrene 1-boronic acid (0.246 g, 1.00mmol), K_2CO_3 (0.151 g , 1.09 mmol) and $PdCl_2(PPh_3)_2$(0.073 g, 0.104mmol) were added to a solution of PS- *b*-P4BrS (0.242 g, 0.025mmol) in 10 mL mixture of THF/H_2O(9: 1). The mixture was refluxed during 29 h . The solvent was removed under reduced pressure, the crude redissolved in ethyl acetate (50 mL) and washed with brine (2 × 25 mL). The solvent was removed under reduced pressure and the dark crude obtained redissolved in THF, filtered and the solvent reduced to circa 3 mL under reduced pressure. The fluorescent copolymer was obtained by precipitation in MeOH as a brownish green solid (0.327 g). ^{1}H NMR (400MHz, $CDCl_3$): 1.30-1.70 (broad m, aliphatic protons), 1.75-2.15 (broad m, aliphatic protons), 2.21-2.30 (m, aliphatic protons), 6.20-6.75 (broad m, ArH), 6.85-7.35 (broad m, ArH),7.68(d, J = 9.2 Hz, ArH),7.90(d, J = 9.2 Hz, ArH),8.04(t, J = 7.6 Hz, ArH), 8.15-8.19 (m, ArH), 8.21 (d, J = 6.8 Hz, ArH), 8.25-8.28 (m, ArH), 8.37 (d, J = 8.0 Hz, ArH) ppm. Mn (GPC) 9576 g^{-1}, Mw (GPC) 10532 g^{-1} with a PDI of 1.10.

Modification of CdTe QDs

CdTe-SAA QDs (λ_{em} = 520 nm) were chemically modified by ligand exchange using 1 -dodecanethiol (1-DDT) as capping agent, to prepare hydrophobic CdTe-DDT QDs, according to the procedure descried by Gaponik et al. [31]. The modification resulted in a redshift of the maximum emission wavelength to 543 nm .

Preparation of the copolymer/QDs nanocomposites for FRET studies

Stock solutions of the donor, PS-b-PS(co-pyren-1-yl), and acceptor, CdTe-DDT QDs, were prepared with concentration of 4mgmL^{-1} and 3.0×10^{-4}M, respectively. The optical properties of the resulting hybrid nanocomposite were measured to calculate FRET.

Characterization

2.6.1. Proton nuclear magnetic resonance (^{1} H NMR) spectroscopy

The fluorescent block copolymer and its precursors were characterized by ^{1}H NMR spectroscopy in terms of their composition and purity. A 400 MHz Avance Bruker NMR spectrometer equipped with an ultrashield magnet and deuterated chloroform ($CDCl_3$) were used in the analysis. The ^{1}H chemical shifts are reported in ppm (parts per million). The residual solvent peak has been used as an internal reference.

Gel permeation chromatography (GPC)

GPC was used to determine the number average molecular weight (M_n) and weight average molecular weight (M_w) of the prepared homo and block copolymers. The samples were prepared in THF (99.9%) and prefiltered on filter plate (hydrophobic polytetrafiuoroethylene, 0.45μ m pore size) before injection. A Waters Alliance GPC Model 2695, equipped with three PLgel MIXED-B columns (inner diameter = 7.5 mm, length = 300 mm and particle size = 10μ m), and a detector Waters 2410 Differential Refractometer were used for the determination. THF was used as eluent with a fiow rate of 1 mL min^{-1} and the temperatures were 25 and 35 °C at the injector and detector, respectively. The M_n, M_w and polydispersity indexes (PDIs) were determined using a calibration curve based on narrow polystyrene standards.

Raman spectroscopy

Room temperature Raman spectra were recorded in a LabRAM HR Evolution spectrometer equipped with a 532 nm laser (Laser Quantum Torus 532, power 50 – 750 mW). The Raman spectra of the samples were acquired in the range 500 – 3500 cm^{-1} (acquisition time: 20 s ; accumulations: 20 ; grating: 600grmm^{-1}; ND filter: 50%; hole: 400). Powder samples were used in the Raman analysis.

Thermogravimetric analysis (TGA)

Thermogravimetric measurements for all prepared materials were carried out using a TA Q500 thermobalance. The samples were heated from 40°C to 900°C, at 10°C · min^{-1}, under a nitrogen flow (60 mL min^{-1}).

Differential scanning calorimetry (DSC)

Thermal properties of the prepared block copolymers were measured using a Netzsch DSC 200 F3 Maia apparatus. The samples were placed in Al pans and heated at 10 °C. min^{-1} from 0 °C to 180°C, under nitrogen flow. Glass transition temperatures (T_g) were taken as the midpoint of the change in heat capacity.

Spectroscopic measurements

UV-Vis absorption spectra of PS-***b***-PS(co-pyren-1-yl) and QDs solutions were acquired on a Shimadzu UV3101PC UV-Vis-NIR spectrophotometer.

Fluorescence experiments were recorded using a Microplate Reader Synergy MX (Bioteck Instruments). The fluorescence quantum yield (Φ_F) of the PS-b-PS(co-pyren-1-yl) and the CdTe QDs in solution, was estimated by comparing the integrated emission of these samples, obtained at one excitation wavelength (λ_{exc} = 360 nm), with that of a standard fluorescent dye, Rhodamine B, in ethanol (Φ_F = 70%) [33]. Stock solutions of the standard, PS-***b*** -PS(co-pyren-1-yl) and CdTe QDs, with similar absorbance (~0.022) at the same excitation wavelength, are assumed to absorb the same number of photons. Thus, a simple ratio of the integrated fluorescence intensities of the standard, PS-b-PS(co-pyren-1-yl) and CdTe QDs solutions provided the Φ_F values. Identical instrument settings for the fluorescent samples and standard solutions were used, and the solvent absorption and emission spectra subtracted.

Scanning transmission electron microscopy (STEM) and energy dispersive X-ray spectroscopy (EDS)

STEM assays were performed to evaluate the morphology of the

CdTe-DDT QDs and the prepared hybrid nanocomposite, using a SEM S360 from Leica equipment, with an acceleration voltage of 15 kV . The samples were prepared by immersion of a copper grid in the solutions, followed by chloroform evaporation at room temperature. X-ray microanalysis was performed with an energy dispersive X-ray Spectrometer (EDS) from Link eXL II from Oxford Instruments attached to the STEM.

Fourier transform infrared (FTIR)

FTIR spectra of the CdTe-DDT QDs, PS-b-PS(co-pyren-1-yl) copolymer and the nanocomposite were recorded in a Jasco spectrometer (Jasco FT/IR 4100). Measurements were performed in a transmittance mode in a spectral range varying from 3500 to 700 cm^{-1}, using 16 scans and a resolution of 4 cm^{-1}. Thin films of each material were prepared after solvent evaporation on the surface of a NaCl solid support and analyzed directly.

Results and discussion

Copolymer

The fluorescent block copolymer PS-b-PS(co-pyren-1-yl) was prepared according to Scheme 1. Initially, PS macroRAFT was synthesized by RAFT polymerization of styrene into BDTB, initiated by AIBN, according to the procedure reported by Abreu et al. [32]. 4bromostyrene was then RAFT polymerized into PS macroRAFT, using AIBN as initiator, giving the block copolymer PS-b-P4BrS. The ratio PS macroRAFT: AIBN: 4BrS = 1: 0.25: 34 resulted in a 82% monomer insertion, according to the M_w determined by GPC. The final synthetic step allowed to produce the PS-b-PS(co-pyren-1-yl), followed by a Suzuki reaction approach to insert the pyrene moieties. The GPC analysis of the obtained material showed a slight increase of the M_W, which is in agreement with the replacement of around 39% of the bromine by pyrene moieties.

The ^{1}H NMR study of the prepared polymers revealed that PS- ***b*** P4BrS displays NMR resonances typical of aliphatic, $1.10 - 2.15$ppm, and aromatic protons, $6.15 - 7.45$ppm. The insertion of pyrene moieties in PS-b-PS(co-pyren-1-yl) was confirmed by the appearance of new resonances typical of aromatic protons at higher chemical shifts (7.45-8.35 ppm).

The insertion of 4-bromostyrene onto PS macroRAFT was further monitored by Raman spectroscopy (Fig. 1). Pristine PS macroRAFT exhibits an intense band at about 1010 cm^{-1} that is assigned to the -CH aromatic stretching vibration. The bands at 2910 cm^{-1} and 3060 cm^{-1} are attributed to the aliphatic -CH and aromatic -CH stretching vibrations, respectively, and the peak at 780 cm^{-1} is attributed to the $C - S$ stretching bond. The spectrum of PS- ***b*** - P4BrS, beyond the characteristic Raman bands of pristine PS macroRAFT, also demonstrate the appearance of a new peak located around 640 cm^{-1} assigned to $C - Br$ bonds, confirming the synthesis of PS- ***b*** - P4BrS. Furthermore, the

increase of the relative intensity of the band at $1075\ cm^{-1}$ in PS- ***b***-P4BrS spectrum indicates that more aromatic rings are present in the chemical structure, thus also confirming the insertion of the 4-bromostyrene units.

Thermal properties of the prepared materials were characterized by DSC and TGA (Fig. 2). TGA analysis of both polymers revealed that the pyrene moiety in PS-b-PS(co-pyren-1-yl) has high influence on the thermal stability when compared to PS- ***b*** P4BrS (Fig. 2A). Both polymers undergo thermal degradation at two different temperatures, where PS-b-PS(co-pyren-1-yl) has a slightly lower thermal stability. While PS-b-P4BrS undergoes almost complete degradation at $374\ ^{\circ}C$, losing 99% of its initial weight, and at $633^{\circ}C$, the remaining residues are eliminated, PS-b-PS(co-pyren-1-yl) has its first degradation step at $343^{\circ}C$, in which
PS macroRAFT PS- PS-PS (co-pyren-1-yl)

Scheme 1. a) PS macroRAFT: AIBN: $4BrS = 1:0.25:34, DMF, N_2, 110\ ^{\circ}C, 42\ h$; b) 40 equivalents (eq.) of pyrene 1-boronic acid, $10\ mol\% PdCl_2(PPh_3)_2, 1.1eq.\ K_2CO_3, THF/H_2O(9:1)$, reflux, 29 h .
losses 86% of its initial weight. At $640\ ^{\circ}C$ occurs the second degradation stage, losing 4% weight. At $900^{\circ}C$ PS-b-PS(co-pyren-1-yl) still has 9% of its initial weight, which is due to the formation of activate porous carbon that results from dehydration, carbonization and oxidation of organic substances [34] that originates char.

From the DSC thermograms (Fig. 2B) it was possible to determine a glass transition temperature (T_g) of $105.6^{\circ}C$ for PS- ***b***-P4BrS, which represents an increase of approximately $30\ ^{\circ}C$ when compared to PS macroRAFT ($77.4\ ^{\circ}C$) [32]. This was an expected result, since the introduction of 4-bromostyrene units not only increases the M_w but also increases the rigidity of the polymer backbone, due to its chemical nature, which are parameters known to have a strong effect on T_g. However, the introduction of pyrene moieties, PS-b-PS(co-pyren-1-yl), do not have a significant influence on T_g. This result might be explained by the contributions of several parameters. Despite the fact that pyrene is rigid and increases the M_w, which may rise the T_g, the low substitution of the bromine groups (39%) means that this moieties will be located along the polymer backbone. This random distribution may introduce bulk spaces between polymer chains, which will endow higher chain mobility and reduce the glass transition temperature [35].

CdTe-DDT quantum dots

The typical photoluminescence (PL) and UV-Vis absorption

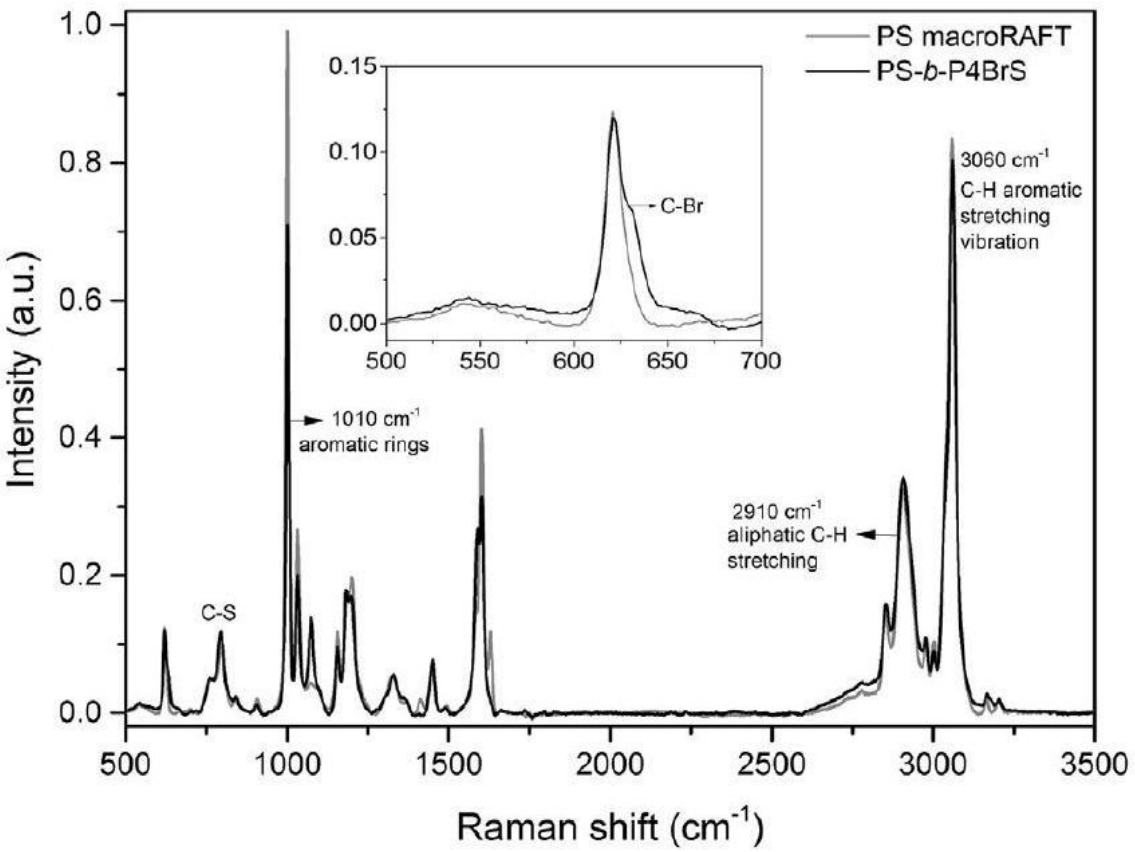

Fig. 1. Raman spectra of PS macroRAFT and PS-b-P4BrS samples. spectra of 1-DDT capped CdTe QDs in chloroform are presented in Fig. 3. According to the PL spectrum, it is possible to observe a symmetric emission peak with a maximum emission wavelength of 543 nm , corresponding to green emission, and a full width at half maximum (FWHM) of approximately 46 nm . The thin FWHM and the PL peak reveal narrow particles size distribution of CdTe-DDT QDs. Using an empirical relationship between the absorption wavelength of the first excitonic peak [36], it was possible to estimate that the CdTe-DDT QDs have a diameter around 2 nm . Furthermore, a broad peak can be noticed in the absorption spectrum, which affords the basic requirement for their application in the energy transfer [10].

According to the procedure described in the experimental section, the Φ_F of PS-b-PS(co-pyren-1-yl) and CdTe-DDT QDs was estimated to be 13% and 19%, respectively, which prompt them as good candidates for several fluorescence applications.

UV absorption spectra of both components were acquired and compared (Fig. 4). The maximum absorption of the block copolymer, PS-b-PS(co-pyren-1-yl), in a concentration of $4.0 \mathrm{mgmL}^{-1}$ was found at 458 nm , which is attributed to the $\pi - \pi^*$ transition of the aromatic chromophores [37], while the absorption spectrum of CdTe-DDT QDs, in a concentration of $43.0 \times 10^{-4} \mathrm{M}$, exhibits a broader and more intense absorption band in the visible region of the spectra ($450 - 550$ nm). Even though both absorption spectra slightly overlap, the latter is red-shifted, displaying the maximum absorption peak at 476 nm . Moreover, the molar extinction coefficient (ε) of PS-b-PS(co-pyren-1-yl) at its maximum absorption wavelength is $6.39 \times 10^3 \mathrm{M}^{-1}\ \mathrm{cm}^{-1}$, smaller than that of CdTe-DDT QDs ($3.20 \times 10^4 \mathrm{M}^{-1}\ \mathrm{cm}^{-1}$). Thus, the broad absorption band of the QDs, associated with

their high ε, make them able to absorb all radiation with higher energy than their first excitonic peak. This improves light absorption and, thus, make them suitable for artificial antenna systems with light harvesting purposes.

Fig. 5 depicts the relationship between the concentration of PS-b-PS(co-pyren-1-yl) and CdTe-DDT QDs and their PL intensity. The obtained results show a similar trend, i.e., PL intensity increases as the concentration increases until a certain value. Above $5.99 mgmL^{-1}$, for PS-b-PS(co-pyren-1-yl), and $4.0 \times 10^{-4}M$, for CdTe-DDT QDs, the PL intensity starts to decline, which is associated to the fluorescence quenching mechanism, induced by selfaggregation of the fluorescent block copolymer or CdTe-DDT QDs, respectively [38]. This phenomenon occurs because both fluorophores are not diluted enough, which induces interchain interactions and therefore, discrete energy levels cannot be achieved [39]. According to this, the dissolution of the aggregates increases the PL intensity, owing to an increased Φ_F of single QDs compared with its aggregated form. Moreover, for high CdTe-DDT QDs

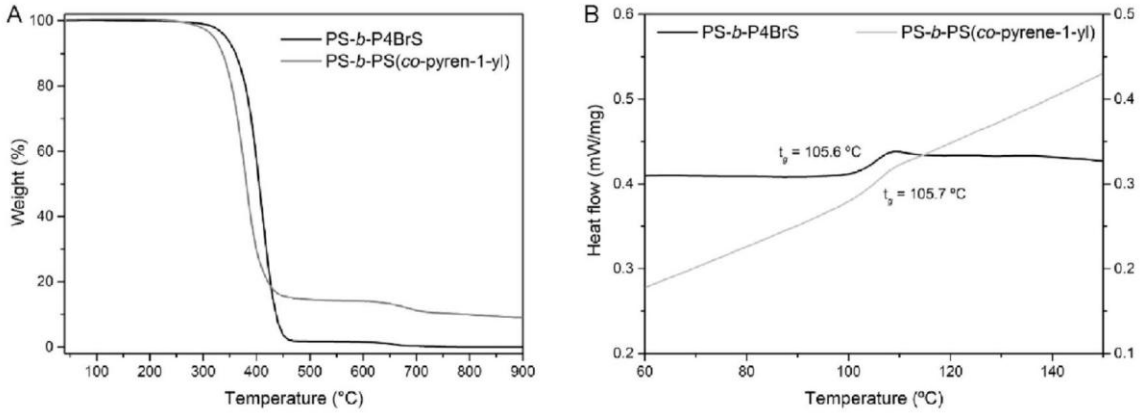

Fig. 2. TGA (A) and DSC (B) thermograms of the block copolymers obtained by RAFT and Suzuki coupling.

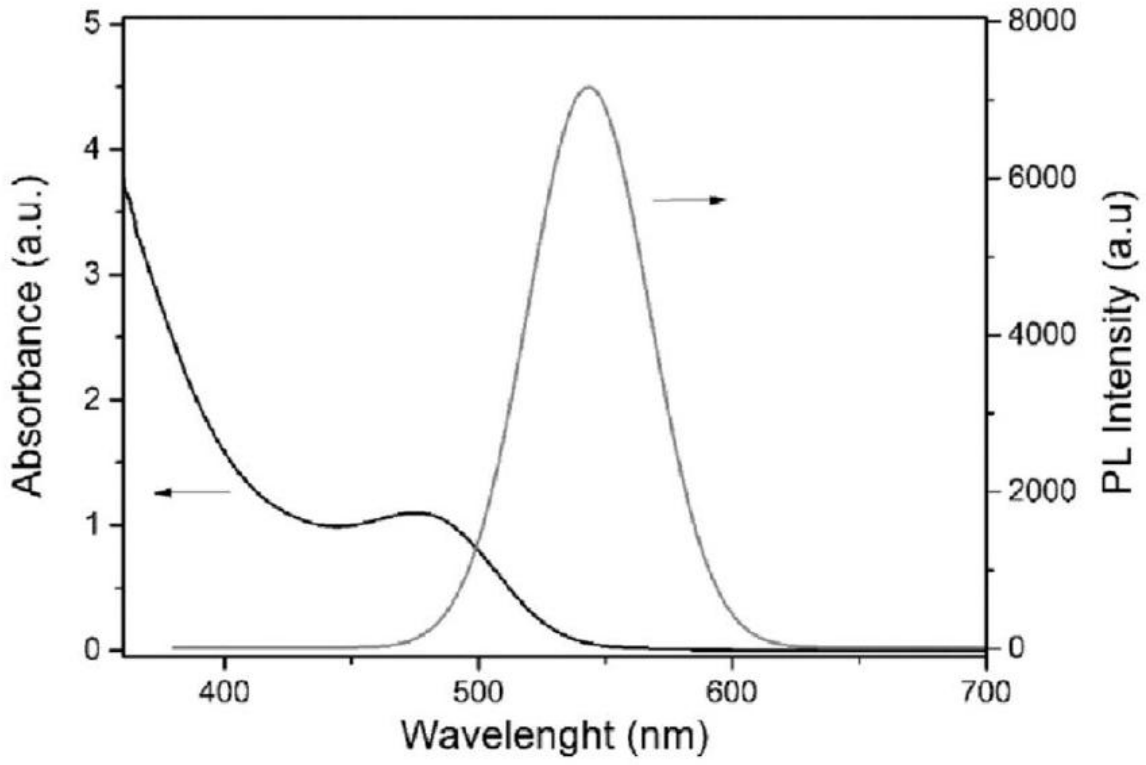

Fig. 3. UV and PL spectra of CdTe-DDT QDs. concentration (5.8×10^{-4}M) it was observed a redshift of the maximum emission wavelength, which can be attributed to the self-absorption of the QDs [40].

The PL spectrum of PS-b-PS(co-pyren-1-yl) and the absorption spectrum of the CdTe-DDT QDs are presented in Fig. 6. As it can be

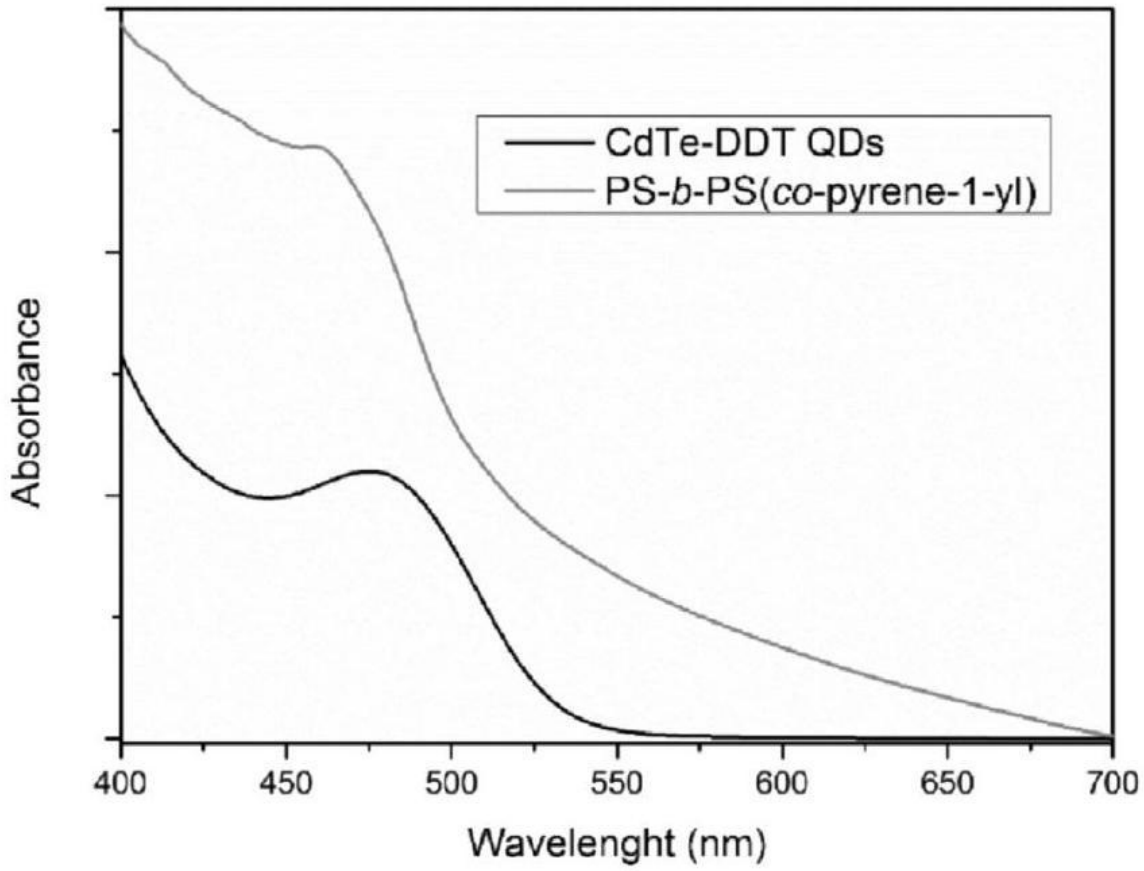

Fig. 4. Absorption spectra of PS- ***b***-PS(co-pyren-1-yl) and CdTe-DDT QDs. observed, combining both results shows a wide overlap between the donor's, [PS-b-PS(co-pyren-1-yl)], PL spectrum and the acceptor's, QDs, absorption spectrum. This is crucial for Förster resonance energy transfer (FRET) phenomenon, allowing a more efficient energy transfer between the fluorophores.

Hybrid nanocomposites

According to Byrne et al. [41], a decrease of the PL intensity is associated with an increase of the number of defects on the QDs' surface, or even to formation of aggregates, which reduces the Φ_F. Therefore, morphological studies of the CdTe-DDT QDs and the resulting hybrid nanocomposite of PS-b-PS(co-pyren-1-yl) and CdTe-DDT QDs were carried out by STEM. Fig. 7A shows the STEM micrograph of the 1-DDT stabilized CdTe QDs, in which is possible to observe well-dispersed nanoparticles, without aggregation and with almost spherical. Accordingly, their size vary from with a size ranging from 4 to 17 nm .

The micrograph depicted in Fig. 7B, evidences the formation of nanoparticles with different sizes, ranging from approximately 4 nm – 20 nm, which are larger than a single QD, since the estimated individual QD diameter is around 2 nm , which can justify a redshift on the PL spectrum. Nevertheless, despite the nanoparticles size, they are well dispersed within the fluorescent block copolymer. These remarks evidence good compatibility between QDs and polymer matrix, where Van der Waals (VdW) forces are expected to be involved in the interparticle interaction, leading to the formation of a coating layer that inhibits the QDs aggregation.

Additionally, energy dispersive x-ray spectroscopy (EDS) was used to confirm the presence of DDT-capped CdTe QDs, within the nanocomposite. The EDS spectrum (Fig. 7C) revealed the presence of cadmium and tellurium, as well as carbon, oxygen and sulfur. Table 1 resumes the energy peaks identified and their corresponding electronic transitions. This analysis confirmed the presence of both fluorophores in the nanocomposite.

The presence of CdTe-DDT QDs dispersed within the PS- ***b*** -PS(co-pyren-1-yl) matrix was also confirmed by FTIR analysis by comparing the spectra of CdTe-DDT QDs, PS-b-PS(co-pyren-1-yl) and CdTe-DDT/PS-b-PS(co-pyren-1-yl) nanocomposite (Fig. 8). The FTIR spectrum of CdTe-DDT QDs (Fig. 8A) exhibits vibrational bands at $3000 - 2800\ cm^{-1}$, attributed to the -CH vibrations of 1-DDT, at $1461\ cm^{-1}$ due to the stretching vibration of $-CH_3$, and a weak band at $750\ cm^{-1}$ assigned to -C-S vibration. For PS-b-PS(co-pyren-1yl) (Fig. 8B), the spectrum revealed a peak around $3026\ cm^{-1}$,

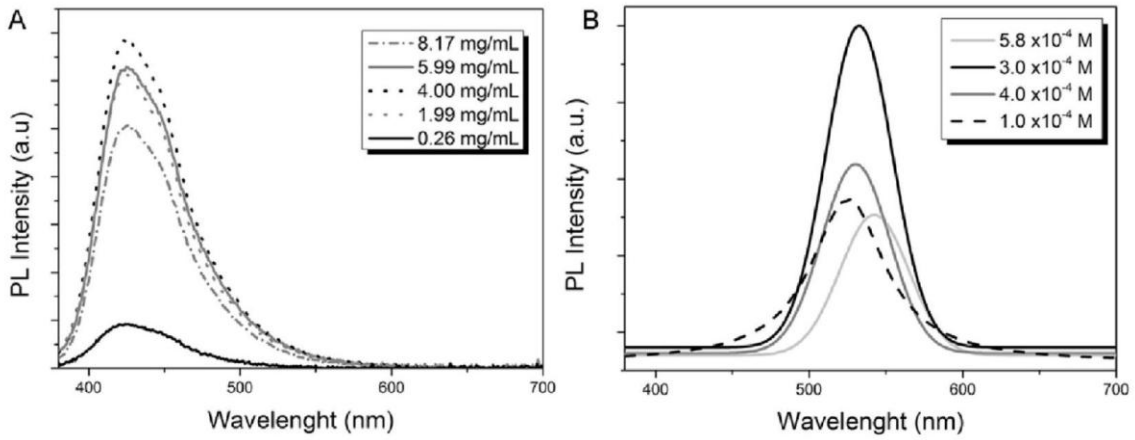

Fig. 5. Normalized PL of PS- ***b***-PS (co-pyren-1-yl) (A) and CdTe-DDT QDs (B) at different concentrations.

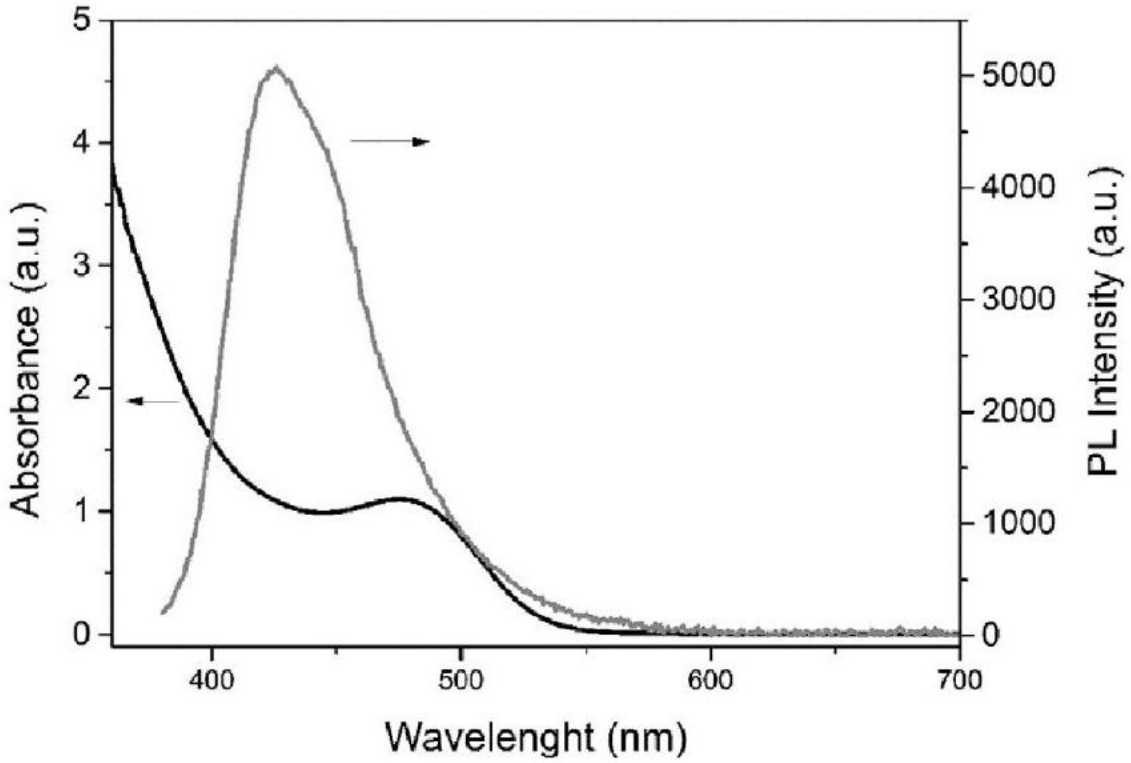

Fig. 6. Absorption and PL spectra of CdTe-DDT QDs and PS-b-PS(co-pyren-1-yl), respectively.

attributed to the aromatic -CH stretching, a vibration between 3000 cm^{-1} and 2800 cm^{-1} assigned to the aliphatic -CH stretching, at 1451 and 1492 cm^{-1} the $C = C$ stretching of the cyclic alkene (aromatic rings), and at 1100 and 756 cm^{-1} vibrations due to the dithioate group (respectively, $C = S$ and $C - S$). The FTIR spectrum of the nanocomposite (Fig. 8C) reveals the characteristic vibration bands of both components, PS-b-PS(co-pyren-1-yl) and CdTe-DDT QDs, with high intensity for all bands, due to the contribution of both species.

Moreover, in the nanocomposite's spectrum it is possible to find the characteristic peaks of PS-b-PS(co-pyren-1-yl) at 1451 and 1492 cm^{-1} and also the one of the CdTe-DDT QDs assigned at 1461 cm^{-1}. Although both compounds display vibrational bands with very close wavenumber (1451 and 1461 cm^{-1}), the presence of QDs in the nanocomposite becomes evident due to the broadening of the vibrational band at 1451 cm^{-1}.

Fig. 9 shows the CdTe-DDT QDs and PS-b-PS(co-pyren-1-yl) PL spectra, in a concentration that results in the maximum PL intensity, respectively 3.0×10^{-4}M and 4.0mgmL^{-1} according to Fig. 4, and the PS- ***b***-PS(co-pyren-1-yl)/CdTe-DDT QDs mixture, in which both components are present in the same concentration as in the individual solutions. Since there is no bleed-through of the acceptor's emission onto the donor's emission, it was possible to calculate FRET for the fluorophores pair by looking at the ratio of the PL peak intensity of the (Fig. 9 c), according to equation (1):

$$E = 1 - \frac{IDA}{ID} \quad (1)$$

where E is the FRET efficiency, I_{DA} is the fluorescence intensity of donor-acceptor and I_D is the fluorescence intensity of the donor.

Even though QDs display negligible FRET using common organic dyes as energy donor [42], the developed system showed a FRET efficiency of 48%. This result revealed that resonance energy was successfully transferred.

The thermal stability of the resulting nanocomposite was evaluated in order to understand the effect of the QDs' dispersion within PS-b-PS(co-pyren-1-yl) (Fig. 10).

The CdTe QDs' thermogram indicates that the DDT in the capping layer decompose in different stages. An initial weight loss at 69°C is attributed to the evaporation of remaining volatiles, and at 145°C occurs the decomposition of dodecanethiol that occurs in two stages, with a combined weight loss of approximately 27%. The thermogram also evidences that the CdTe inorganic core corresponds to 60% of the initial material, based on the amount of remaining residue at 900°C.

Nevertheless, when the QDs were dispersed within the PS- ***b*** -PS(co-pyren-1-yl) matrix, the system exhibits higher thermal stability, due to the block copolymer shell. Herein, upon an initial evaporation of volatiles, occurs the first degradation stage of DDT at 173°C, an enhancement of the thermal stability that was expected, with a weight loss of 9.2%. This observation reveals that the block copolymer has a significant effect in the nanoparticles' decomposition. Above 316 °C, the nanocomposite reveals a major weight loss, around 68.62%, which is due the second degradation stage of DDT overlapped with the degradation of the fluorescent block copolymer. Furthermore, from the nanocomposite's thermogram, it is observed a slight higher thermal stability around 370 °C, revealing that the dodecanethiol ligands induce suitable colloidal stability and generate a barrier effect that retard the thermal transport during the block copolymer decomposition. Herein, high surface areas and enhanced interaction, through VdW forces, between the copolymer chains and the organic ligand from the CdTe core are expected. This interaction can limit the mobility of the QDs within the copolymer matrix, resulting in higher thermal stability of the nanocomposite.

The nanocomposite thermogram also reveals a low CdTe

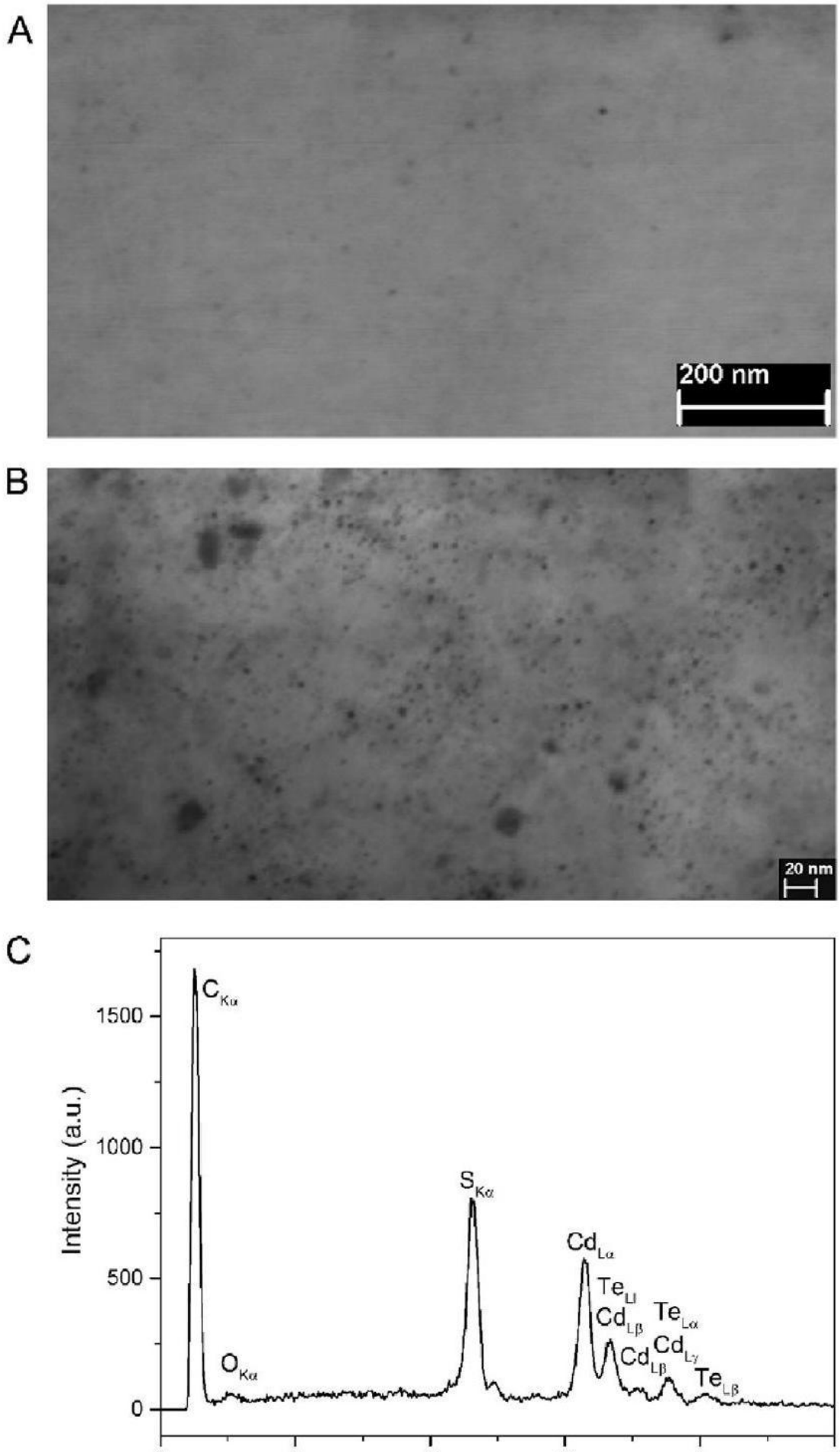
A
200 nm
B
20 nm
C
Intensity (a.u.)
1500
1000
500
0
$C_{K\alpha}$
$O_{K\alpha}$
$S_{K\alpha}$
$Cd_{L\alpha}$
$Te_{L\beta}$
$Cd_{L\beta}$
$Te_{L\alpha}$
$Cd_{L\gamma}$
$Cd_{L\beta}$
$Te_{L\beta}$

Fig. 7. STEM micrographs of CdTe-DDT QDs (A) and nanocomposite (B) and EDS spectrum (C) of the nanocomposite.

Table 1
Energy peaks and respective electronic transition in the nanocomposite's EDS spectrum.

Element	Transition	Energy (KeV)
C	K_{α}	0.277
O	K_{α}	0.525
S	K_{α}	2.307
Cd	L_{α}	3.130
	L_{β}	3.317; 3.528
	L_{γ}	3.717
Te	L_{1}	3.336
	L_{α}	3.759
	L_{β}	4.030

inorganic core content, which is due to the small amount of QDs in the mixture. Additionally, it is observed a higher degradation of the copolymer at high temperature, since just 3% of remain material is found at 900°C, which is not observed in the PS-b-PS(co-pyren-1-

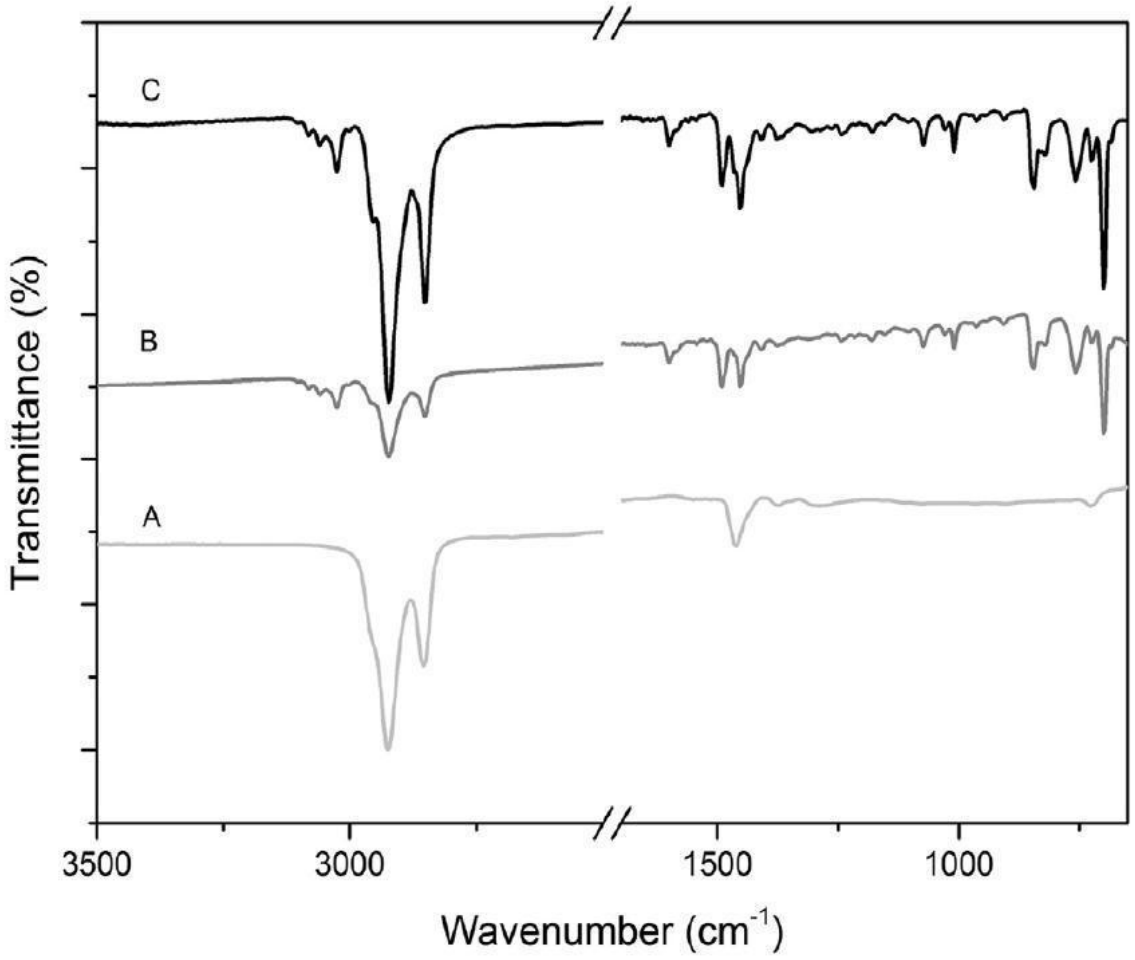

Fig. 8. FTIR spectra of CdTe-DDT QDs (A), PS- ***b***-PS(co-pyren-1-yl) block copolymer (B) and nanocomposite based on PS-b-PS(co-pyren-1-yl) and CdTe-DDT QDs (C).

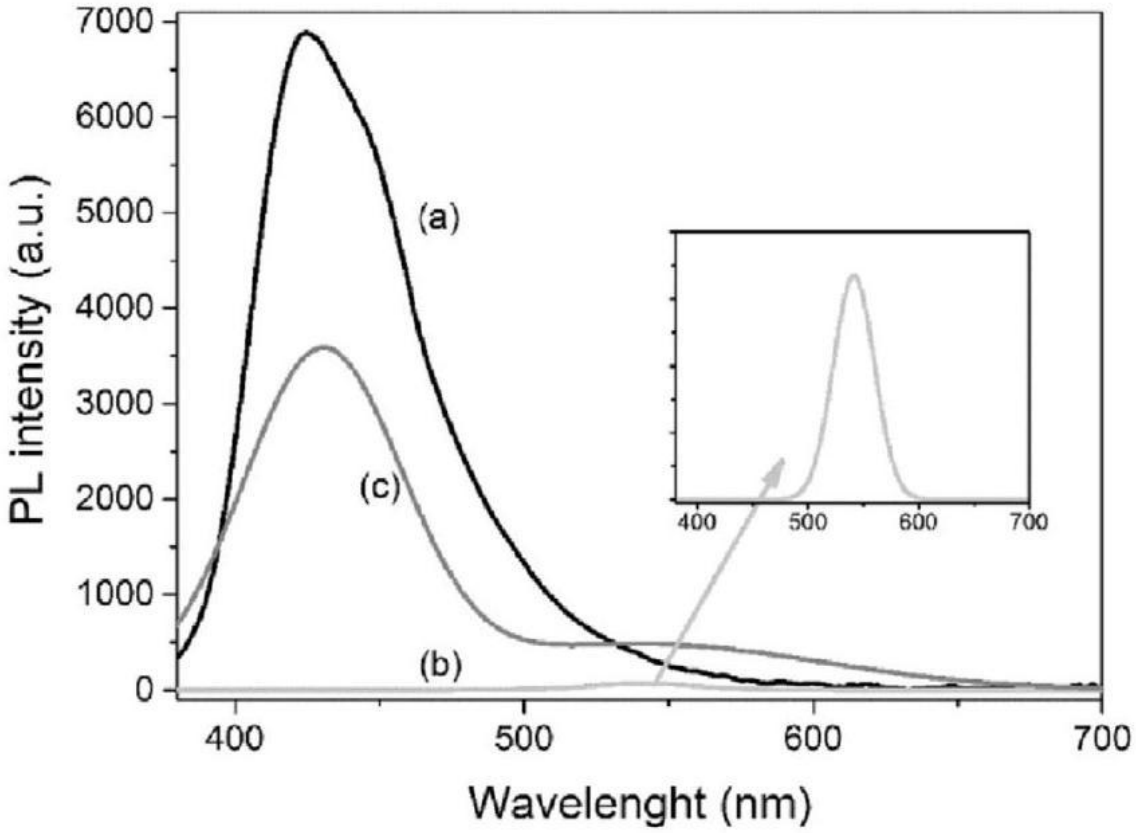

Fig. 9. PL spectra of PS-b-PS(co-pyren-1-yl) (a), CdTe-DDT (b), and the mixture of both (c).

yl) thermogram (Fig. 2A). This behavior can be related to the presence of the CdTe inorganic core. It is well known that Cd can be used as catalyst in several chemical reactions [43], thus we suspect that, in our case, it can catalyze the degradation of the products that are being formed during the copolymer's pyrolysis.

Conclusions

A fluorescent block copolymer, PS- ***b***-PS(co-pyren-1-yl), whose fluorescence is due to the presence of pyrene moieties, was successfully synthesized. The PS-b-P4BrS was obtained with good conversion yield, following a RAFT polymerization strategy. A Suzuki cross coupling reaction allowed to insert several pyrene units onto PS-b-P4BrS. Fluorescence assays performed for the fluorescent block copolymer allowed to determine a Φ_F of 13%. Combining the copolymer and CdTe-DDT QDs resulted in a nanocomposite that proved to be able to successfully experience resonance energy transfer, FRET. In this system, CdTe-DDT QDs were able to participate as energy acceptors, with an efficiency of 48%.

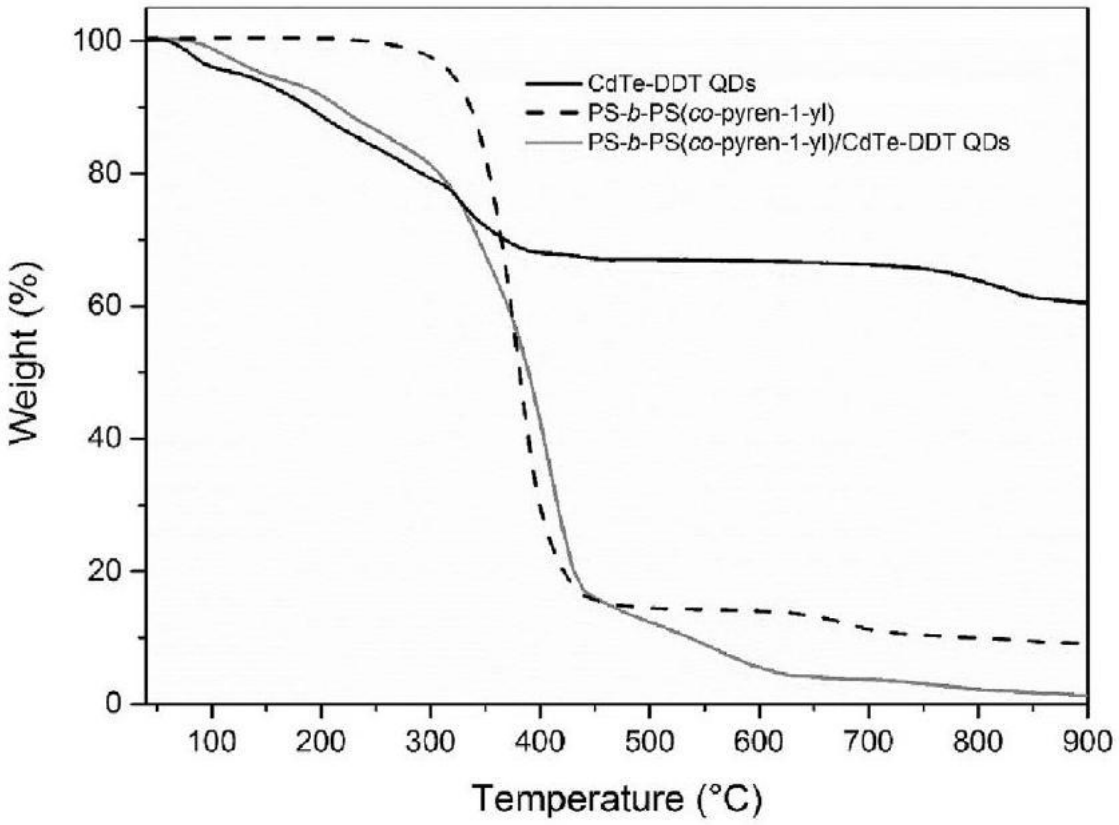

Fig. 10. Thermogravimetric analysis of PS- ***b***-PS(co-pyren-1-yl), CdTe-DDT QDs, and PS-***b***-PS(co-pyren-1-yl)/CdTe-DDT nanocomposite.

Additionally, the QDs as part of the nanocomposite showed higher thermal stability when compared to the QDs themselves. The results obtained indicate that this new material has great potential for application in light harvesting systems.

Acknowledgements

Isabel Moura and Arsénio de Sá contributed equally to this work. The authors acknowledge n-STeP - Nanostructured systems for Tailored Performance, with reference NORTE-07-0124-FEDER000039, supported by the Programa Operacional Regional do Norte (ON.2). This work is funded by FEDER funds through the COMPETE 2020 Programme and National Funds through FCT - Portuguese Foundation for Science and Technology under the project UID/CTM/ 50025/2013, with the grant references IPC/AVM/14/2015 and IPC/ AVM/22/2015.

References

[1] Pingping L, Shaopu L, Shuguang Y, Xiaoqing F, Youqiu H. A sensitive sensor for anthraquinone anticancer drugs and hsDNA based on CdTe/CdS quantum dots fluorescence reversible control. Colloids Surf A Physicochem Eng Asp 2011;392(1):7-15.
[2] Razykov TM, Ferekides CS, Morel D, Stefanakos E, Ullal HS, Upadhyaya HM. Solar

photovoltaic electricity: current status and future prospects. Sol Energy 2011;85(8):1580-608.
[3] Cao, Banin U. Growth and properties of semiconductor core/shell nanocrystals with InAs cores. J Am Chem Soc 2000;122(40):9692-702.
[4] Wang YA, Li JJ, Chen H, Peng X. Stabilization of Inorganic nanocrystals by organic dendrons. J Am Chem Soc 2002;124(10):2293-8.
[5] Gaponik N, Radtchenko IL, Sukhorukov GB, Weller H, Rogach AL. Toward encoding combinatorial libraries: charge-driven microencapsulation of semiconductor nanocrystals luminescing in the visible and near IR. Adv Mater 2002;14(12):879-82.
[6] Hu MZ, Zhu T. Semiconductor nanocrystal quantum dot synthesis approaches towards large-scale industrial production for energy applications. Nanoscale Res Lett 2015;10:469.
[7] Ma H, Bai X, Zheng L. Self-assembly of CdTe QDs into urchin-like microspheres by the assistance of a long-chain ionic liquid monolayer. CrystEngComm 2011;13(11):3788-93.
[8] Larson DR, Zipfel WR, Williams RM, Clark SW, Bruchez MP, Wise FW, et al. Water-soluble quantum dots for multiphoton fluorescence imaging in vivo. Science 2003;300(5624):1434-6.
[9] Wang M, Oh JK, Dykstra TE, Lou X, Scholes GD, Winnik MA. Surface modification of CdSe and CdSe/ZnS semiconductor nanocrystals with poly(N,Ndimethylaminoethyl methacrylate). Macromolecules 2006;39(10):3664-72.
[10] Huang W, Li L, Hui G, Chen D, Zhong A. Fluorescent polymer with CdTe quantum dots and 1,8-naphthahmide fluorescent polymer: synthesis, characterization, and FRET. J Appl Polym Sci 2013;129(3):1256-63.
[11] Wagh A, Qian SY, Law B. Development of biocompatible polymeric nanoparticles for in vivo NIR and FRET imaging. Bioconjug Chem 2012;23(5):

981-92.
[12] Algar WR, Wegner D, Huston AL, Blanco-Canosa JB, Stewart MH, Armstrong A, et al. Quantum dots as simultaneous acceptors and donors in time-gated Förster resonance energy transfer relays: characterization and biosensing. J Am Chem Soc 2012;134(3):1876-91.
[13] Clapp AR, Medintz IL, Fisher BR, Anderson GP, Mattoussi H. Can luminescent quantum dots be efficient energy acceptors with organic dye donors? J Am Chem Soc 2005;127(4):1242-50.
[14] Sapsford KE, Berti L, Medintz IL. Materials for fluorescence resonance energy transfer analysis: beyond traditional donor-acceptor combinations. Angew Chem Int Ed Engl 2006;45(28):4562-89.
[15] Kochuveedu ST, Son T, Lee Y, Lee M, Kim D, Kim DH. Revolutionizing the FRETbased light emission in core-shell nanostructures via comprehensive activity of surface plasmons. Sci Rep 2014;4:4735.
[16] Wu W-C, Chen C-Y, Tian Y, Jang S-H, Hong Y, Liu Y, et al. Enhancement of aggregation-induced emission in dye-encapsulating polymeric micelles for bioimaging. Adv Funct Mater 2010;20(9):1413-23.
[17] Yao H, Zhang Y, Xiao F, Xia Z, Rao J. Quantum dot/bioluminescence resonance energy transfer based highly sensitive detection of proteases. Angew Chem Int Ed Engl 2007;46(23):4346-9.
[18] Hoffman JB, Choi H, Kamat PV. Size-dependent energy transfer pathways in CdSe quantum dot-squaraine light-harvesting assemblies: förster versus dexter. J Phys Chem C 2014;118(32):18453-61.
[19] Zhang H-M, Wang Y-Q, Jiang M-L. A fluorimetric study of the interaction of C.I. Solvent Red 24 with haemoglobin. Dyes Pigm 2009;82(2):156-63.
[20] Higgins C, Lunz M, Bradley AL, Gerard VA, Byrne S, Gun'ko YK. FRET in

selfassembled CdTe quantum dot nanoclusters. in 2010 12th International Conference on Transparent Optical Networks, 2010.
[21] Lin YC, Chou WC, Susha AS, Rogach AL. Förster resonance energy transfer in mixed-size CdTe quantum dots with optimized donor-acceptor concentration ratio. In: Proc. SPIE 7937, ultrafast phenomena in semiconductors and nanostructure materials XV; 2011.
[22] Li M, Li F, He Z, Zhang J, Han J, Lu P. Two-photon-excited fluorescence resonance energy transfer in an aqueous system of CdTe quantum dots and Rhodamine B. J Appl Phys 2014;116(23):233106.
[23] Feng Y, Liu L, Hu S, Zou P, Zhang J, Huang C, et al. Efficient fluorescence energy transfer system between fluorescein isothiocyanate and CdTe quantum dots for the detection of silver ions. Luminescence 2016;31(2):356-63.
[24] Kundu S, Patra A. Nanoscale strategies for light harvesting. Chem Rev 2017;117(2):712-57.
[25] Ramachandra S, Popovic' ZD, Schuermann KC, Cucinotta F, Calzaferri G, De Cola L, et al. Förster resonance energy transfer in quantum dot-dye-loaded zeolite 1 nanoassemblies. Small 2011;7(10):1488-94.
[26] Qiao J, Qi L, Shen Y, Zhao L, Qi C, Shangguan D, et al. Thermal responsive fluorescent block copolymer for intracellular temperature sensing. J Mater Chem 2012;22(23):11543-9.
[27] Yang H, Paek K, Kim BJ. Efficient temperature sensing platform based on fluorescent block copolymer-functionalized graphene oxide. Nanoscale 2013;5(13):5720-4.
[28] Rogach AL. Fluorescence energy transfer in hybrid structures of semiconductor nanocrystals. Nano Today 2011;6(4):355-65.
[29] Figueira-Duarte Teresa M, Müllen K. Pyrene-based materials for organic electronics. Chem Rev 2011;111(11):7260-314.
[30] Wang G, Chang X, Peng J, Liu K, Zhao K, Yu C, et al. Towards a new FRET system via combination of pyrene and perylene bisimide: synthesis, selfassembly and fluorescence behavior. Phys Chem Chem Phys 2015;17(7): 5441-9.
[31] Gaponik N, Talapin DV, Rogach AL, Eychmüller A, Weller H. Efficient phase transfer of luminescent thiol-capped nanocrystals: from water to nonpolar organic solvents. Nano Lett 2002;2(8):803-6.
[32] Abreu AS, Oliveira M, Rodrigues PV, Moura I, Botelho G, Machado AV. Synthesis and characterization of polystyrene-block-poly(vinylbenzoic acid): a promising compound for manipulating photoresponsive properties at the nanoscale. J Mater Sci 2015;50(7):2788-96.
[33] López F, Ojeda P, Arbeloa I. Fluorescence self-quenching of the molecular forms of rhodamine B in aqueous and ethanolic solutions. J Luminesc 1989;44:105-12.
[34] Hasegawa G, Kanamori K, Nakanishi K, Hanada T. Fabrication of activated carbons with well-defined macropores derived from sulfonated poly(divinylbenzene) networks. Carbon 2010;48(6):1757-66.
[35] Shenhar R, Sanyal A, Uzun O, Rotello VM. Anthracene-functionalized polystyrene random copolymers: effects of side-chain modification on polymer structure and behavior. Macromolecules 2004;37(1):92-8.
[36] Yu WW, Qu L, Guo W, Peng X. Experimental determination of the extinction coefficient of CdTe, CdSe and CdS nanocrystals. Chem Mater 2003;15: 2854-60.
[37] Li Z, Li P, Huang J. Synthesis of amphiphilic copolymer brushes: poly(ethylene oxide)-graft-polystyrene. J Polym Sci Part A Polym Chem 2006;44(15): 4361-71.
[38] Bai F, Mo Y, Wang Z, Chen D, Li G, Hu H. Fluorescence quenching study on some substituted polysilanes. Polym Adv Technol 1996;7(2):92-4.
[39] Jakubiak R, Collison CJ, Wan WC, Rothberg LJ, Hsieh BR. Aggregation quenching of

luminescence in electroluminescent conjugated polymers. J Phys Chem A 1999;103(14):2394-8.
[40] Zhang W, Dai D, Chen X, Guo X, Fan J. Red shift in the photoluminescence of colloidal carbon quantum dots induced by photon reabsorption. Appl Phys Lett 2014;104(9):091902.
[41] Byrne SJ, Corr SA, Rakovich TY, Gun'ko YK, Rakovich YP, Donegan JF, et al. Optimisation of the synthesis and modification of CdTe quantum dots for enhanced live cell imaging. J Mater Chem 2006;16(28):2896-902.
[42] Delehanty JB, Medintz IL, Pons T, Brunel FM, Dawson PE, Mattoussi H. Selfassembled quantum dot-peptide bioconjugates for selective intracellular delivery. Bioconjugate Chem 2006;17(4):920-7.
[43] Mukherjee S, Ghosh SK. Cadmium-based catalysts. Sustainable catalysis: with non-endangered metals Part 2. 2015. p. 91